Artificial Intelligence in Agriculture 10 (2023) 46–60

Contents lists available at ScienceDirect

Artificial Intelligence in Agriculture

journal homepage: http://www.keaipublishing.com/en/journals/artificial-intelligence-in-agriculture/

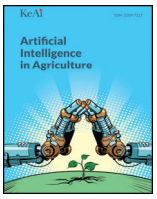

Cumulative unsupervised multi-domain adaptation for Holstein cattle re-identification

Fabian Dubourvieux [a,b,*,1], Guillaume Lapouge [a,*,1], Angélique Loesch [a], Bertrand Luvison [a], Romaric Audigier [a]

[a] Université Paris-Saclay, CEA List, Palaiseau 91120, France
[b] LITIS, INSA Rouen, Normandie Université, Saint-Etienne-du-Rouvray 76801, France

ARTICLE INFO

Article history:
Received 26 May 2023
Received in revised form 1 October 2023
Accepted 7 October 2023
Available online 17 October 2023

Keywords:
Re-identification
Domain adaptation
Holstein cattle
Unsupervised learning
Monitoring

ABSTRACT

In dairy farming, ensuring the health of each cow and minimizing economic losses requires individual monitoring, achieved through cow *Re*-Identification (Re-ID). Computer vision-based Re-ID relies on visually distinguishing features, such as the distinctive coat patterns of breeds like Holstein.

However, annotating every cow in each farm is cost-prohibitive. Our objective is to develop *Re*-ID methods applicable to both labeled and unlabeled farms, accommodating new individuals and diverse environments. Unsupervised Domain Adaptation (UDA) techniques bridge this gap, transferring knowledge from labeled source domains to unlabeled target domains, but have only been mainly designed for pedestrian and vehicle *Re*-ID applications.

Our work introduces Cumulative Unsupervised Multi-Domain Adaptation (CUMDA) to address challenges of limited identity diversity and diverse farm appearances. CUMDA accumulates knowledge from all domains, enhancing specialization in known domains and improving generalization to unseen domains. Our contributions include a CUMDA method adapting to multiple unlabeled target domains while preserving source domain performance, along with extensive cross-dataset experiments on three cattle *Re*-ID datasets. These experiments demonstrate significant enhancements in source preservation, target domain specialization, and generalization to unseen domains.

1. Introduction

Traditionally, farmers have shouldered the vital responsibility of overseeing the health and behavior of their dairy cows. Detecting early indicators of heat or unusual behavior in these animals is of paramount importance, not only to ensure their overall well-being but also to mitigate potential economic losses. As we transition from manual monitoring to computer vision-based individual tracking, there arises the need for precise identification of each cow within a farm. This intricate task is commonly referred to as cow *Re*-Identification (Re-ID). In this paper, we focus the cow Re-ID on the Holstein breed, notable for its visually distinctive spot patterns. Besides, we match observations of the same individual in the short term, i.e. over a defined timeframe during which its visual appearance is presumed to remain unchanged.

Historically, *Re*-ID has been a focal point in image interpretation, particularly in the context of pedestrian video surveillance Zheng et al. (2016). The primary objective of *Re*-ID in this context is to track or retrieve individuals of interest through camera networks with non-overlapping fields of view. The introduction of supervised learning, facilitated by deep Convolutional Neural Networks (CNNs) Krizhevsky et al. (2012), has significantly advanced the performance of supervised person *Re*-ID Ye et al. (2021).

The *Re*-ID paradigm has expanded beyond pedestrian tracking to encompass a broader array of real-world applications, including vehicle *Re*-ID for traffic surveillance Khan and Ullah (2019) and animal *Re*-ID for monitoring cattle Schneider et al. (2020); Liu et al. (2019a, 2019d, 2019b).

Supervised *Re*-ID demands the painstaking annotation of datasets. In the specific context of cow Re-ID, the impracticality and cost of annotating every cow in each farm necessitate the development of a *Re*-ID method capable of generalizing effectively across both labeled and unlabeled farms. This adaptability is crucial to accommodate the introduction of new cows into established farms and the deployment of the technology in novel farm environments. However, *Re*-ID grapples with a notable decline in performance when the test image distribution diverges from that of the training dataset.

To address these challenges, Unsupervised Domain Adaptation (UDA) methods have been devised for Re-ID Ge et al. (2019, 2020);

* Corresponding authors at: Université Paris-Saclay, CEA List, Palaiseau 91120, France.
E-mail address: guillaume.lapouge@cea.fr (G. Lapouge).
[1] These authors contributed equally to this work.

https://doi.org/10.1016/j.aiia.2023.10.002

Dubourvieux et al. (2021a). UDA seeks to adapt a model to a domain of interest by leveraging an annotated dataset from another domain (the source domain) and unlabeled data from the domain of interest (the target domain). While extensively explored for pedestrian and vehicle *Re*-ID, UDA proves particularly relevant in cow Re-ID applications, given the impracticality of annotating each cow in numerous farms.

However, the unique constraints and requirements inherent in the cow Re-ID application have spurred further developments, which form the core focus of this paper. In cow *Re*-ID, each farm represents a distinct domain, characterized by its unique set of individuals, cameras, and environmental context. Consequently, cross-domain performance degradation becomes a pertinent issue. Additionally, each domain typically comprises a limited subset of animals, restricting the generalization potential of *Re*-ID networks trained on individual datasets, as in conventional UDA.

In pursuit of enhancing the model's discriminatory capabilities among cows, we propose a novel framework: Cumulative Unsupervised Multi-Domain Adaptation (CUMDA). CUMDA aims to accumulate *Re*-ID knowledge from data collected across multiple farms (diverse domains), enabling superior specialization within known domains and improved performance when confronted with previously unseen domains.

To our knowledge, existing UDA Re-ID methods have primarily focused on multi-domain scenarios with multiple annotated source domains. No UDA Re-ID approach has been designed specifically for multiple unlabeled target domains. Moreover, while the Domain Generalization framework Wang et al. (2021) seeks to create models that perform well on unseen target domains, it differs from CUMDA. CUMDA assumes knowledge of all target domains during training and access to unlabeled data from these domains, with the objective of enhancing specialization and cross-domain *Re*-ID performance through knowledge accumulation. While generalization is not the primary aim, we anticipate that a CUMDA model, through the accumulation of knowledge from diverse target domains, can enhance its generalization to previously unseen domains.

Furthermore, traditional UDA frameworks often prioritize maximizing performance on the target domain at the expense of forgetting or neglecting source domain knowledge Dubourvieux et al. (2021a). In practice, when new cameras are deployed on a farm, the adaptation of the *Re*-ID model to these new devices is desired, while maintaining high performance on existing ones—a characteristic we term"source conservation."

In summary, while existing *Re*-ID methods may be directly applicable to cattle *Re*-ID, none of them fully addresses the unique constraints and practical requirements of cow Re-ID that underscore the choice of a CUMDA framework over a conventional UDA approach. Driven by these practical considerations and the need for cross-domain cattle Re-ID solutions, this paper endeavors to design a cross-domain model tailored to the distinctive challenges of cattle Re-ID across multiple farms, an area that has seen limited study. Our aim is to develop such a method within the framework of CUMDA, emphasizing source conservation and the accumulation of knowledge from multiple unsupervised target domains. This paper comprises two primary contributions:

- A Source-Guided CUMDA method, that can improve cross-domain re-ID performance, on one or multiple target domains, while being able to accumulate knowledge from multiple domains and preserve the source performance.
- Extensive cross-dataset experiments for CUMDA re-ID on 2 public cow re-ID datasets and a private one.

2. Related work

This work is at the intersection of two research areas: cattle re-ID and cross-domain re-ID.

2.1. Cattle re-ID

Re-ID has been mainly focused on pedestrian and vehicles Ye et al. (2021). Some work exists for animal re-ID, focusing for instance on Amur tiger re-ID Liu et al. (2019a); Li et al. (2019a); Liu et al. (2019d). Nevertheless, Amur tigers have a coat of spots visually very distinct from cows, as well as the deformations of these spots their movements specific to their morphology. This leads us to believe that cows have a sufficiently distinct appearance from Amur tigers to be considered a distinct class of interest for re-ID Liu et al. (2019d). That's why he specificity of the appearance of cows has led to specific works Bergamini et al. (2018); Andrew et al. (2021, 2016, 2017); Gao et al. (2021), studying it under the frameworks of supervised learning or self-supervised learning Gao et al. (2021) assuming access to tracklets. However, supervised learning or self-supervised learning are not suitable for learning combining data from multiple farms, due to the increased annotation cost for the supervised paradigm or the failure to account for inter-domain heterogeneities with multiple farm data in the self-supervised framework. To the best of our knowledge, cattle re-ID has therefore never focused on the cross-domain setting nor the multiple-domain one.

2.2. Cross-domain person and vehicle re-ID via UDA paradigm

Cross-domain re-ID has been extensively studied for people and vehicle re-ID problems. It can be divided into two main families of approaches.

Domain-translation approaches were the first ones considered for cross-domain person re-ID. Among these approaches, *image-to-image translation* methods seek to transfer the source images into the target domain style Wei et al. (2018a); Bak et al. (2018); Deng et al. (2018); Zhong et al. (2018); Liu et al. (2019c); Huang et al. (2019); Chen et al. (2019); Li et al. (2019b). They are based on generative models such as the CycleGAN Zhu et al. (2017). They are constrained during training to translate images to new style while preserving the identity class. This allows the identity label to be reused for supervised re-ID learning from labeled source images with a new target-style. *Domain-invariant feature learning* methods Wang et al. (2018); Lin et al. (2018); Chang et al. (2019b); Li et al. (2018, 2019b); Qi et al. (2019) directly constrain the feature space of the learned model, e.g. by aligning feature distributions between domains, with the objective that the re-ID model learned to be discriminative on the source domain, is also discriminative on the target domain in this domain-invariant space.

Because of limited cross-domain performance of domain-translation approaches, researchers have been interested in *pseudo-labeling* approaches Song et al. (2020); Zhang et al. (2019); Jin et al. (2020); Tang et al. (2019); Zhai et al. (2020a); Zou et al. (2020); Fu et al. (2019). They consist in predicting identity labels for images of the target domain, by clustering features obtained with an initial feature encoder, generally learned to perform re-ID in a supervised way on the source domain. Pseudo-label approaches have allowed a clear improvement of the cross-domain re-ID performance Ge et al. (2019, 2020); Dubourvieux et al. (2021b, 2022). To achieve even better performance, techniques have been developed to get better pseudo-labels or make the framework more robust against noisy labels Chen et al. (2020); Zhai et al. (2020b); Zhao et al. (2020); Peng et al. (2020); Yu et al. (2019); Zhong et al. (2019); Luo et al. (2020); Dubourvieux et al. (2021a).

The approach proposed in this paper is also in line with pseudo-labeling approaches. Contrary to existing work, this one focuses on a new class of objects for cross-domain re-ID, the cross-domain cow re-ID, for which no UDA approach has been considered. Moreover, unlike existing work in pseudo-labeling for cross-domain person re-ID, which considers a single target domain scenario, this work tackles a more challenging, yet practical and more specific to cattle re-ID real-world requirements, cross-domain problem: Cumulative Unsupervised Multi-Domain Adaptation (CUMDA). This cross-domain framework

seeks to leverage the knowledge from one or several domains of interest (e.g.: various cattle farms), to improve the cross-domain re-ID performance for each domain (each farm), including on the source domain re-ID ability of the model.

3. Methodology

Lower part: proposed pseudo-labeling method for multi-target CUMDA re-ID. Black arrows indicate the pseudo-labeling and training cycle, gray arrows indicate the clustering parameters optimization steps. It considers a set of n target domains $\mathcal{T}_1, \ldots, \mathcal{T}_n$ and a source domain $\mathcal{S}$. For each target, *SOURCE CALIBRATION* computes an associated labeled source validation set $\left\{x_{val}^{\mathcal{S}_1}\right\}, \ldots, \left\{x_{val}^{\mathcal{S}_n}\right\}$. After *FEATURE EXTRACTION* of all source validation and target sets, *SOURCE-GUIDED AUTO HP TUNING* computes target-specific optimal hyperparameter (HP) values $\lambda_1^*, \ldots, \lambda_n^*$ from calibrated source validation sets by maximizing clustering quality $\mathcal{Q}$ (Sec. 3.4). Target-specific *PSEUDO LABELING BY CLUSTERING* is then carried out. *TRAINING* is jointly done on all pseudo-labeled target sets and on the labeled source domain by minimizing $L_{SG-CUMDA}$ (Sec. 3.2).

Our goal is to design a CUMDA re-ID method that can improve re-ID performance on all seen domains. More specifically, it is expected that this method can:

- specialize for one or multiple target domains to improve performance on them;
- ensure good performance on the source domain.

We also expect such a model to generalize well on an unseen new target domain, as it should accumulate knowledge from multiple domains.

As illustrated in the upper part of Fig. 1, existing pseudo-labeling methods are designed for UDA re-ID, i.e. to improve re-ID performance on a single target domain, using only data from this domain. Therefore, they need to be rethought in order to meet the previously mentioned objectives of CUMDA re-ID, and to incorporate the use of data from multiple domains. This section introduces key elements of our CUMDA re-ID method.

The lower part introduces our CUMDA re-ID method whose components will be motivated in this section.

General notations. We consider a set of n target domains of interest $\mathcal{T}_1, \ldots, \mathcal{T}_n, n \in \mathrm{N}$ and a source domain $\mathcal{S}$, from which a set of labeled data S from $\mathcal{S}$, and unlabeled data $T_1, \ldots, T_n$ from $\mathcal{T}_1, \ldots, \mathcal{T}_n$ (the target domains) are available.

3.1. Pseudo-labeling by clustering

A feature encoder $f_\theta, \theta \in \mathrm{R}^p, p \in \mathrm{N}$ (usually a CNN) is trained on the labeled source dataset T, by minimizing a re-ID loss function (e.g.: Classification Loss, Triplet Loss as in Hermans et al. (2017), a combination of both as in Luo et al. (2019)…) $L_{ID}(\theta, T)$, w.r.t θ. Then, a clustering function C_λ defined by hyperparameters (HP) $\lambda \in \mathrm{R}^m, m \in \mathrm{N}$ is used to predict pseudo-labels of data samples in each target set, by using the feature representation of their data. Pseudo-labeled target sets $\widehat{T}_1, \ldots, \widehat{T}_n$ can then be obtained:

$$\forall k \in [1, n], \quad \widehat{T}_k = C_\lambda(f_\theta, T_k) \tag{1}$$

This step, described by Eq. 1, is called Pseudo-Labeling by Clustering (PLC). These pseudo-labels will be used to define the loss that supervises the learning on the targets.

3.2. Source-guided CUMDA re-ID learning

The objectives of CUMDA re-ID are being able to improve the cross-domain performance for one or multiple target domains, while being able to preserve the source re-ID performance. Inspired by the source-guided loss function designed by Dubourvieux et al. (2021a) for single-target domain UDA re-ID, we define a new Source-Guided loss function extended for CUMDA re-ID. Therefore, f_θ is fine-tuned by minimizing a Source-Guided CUMDA (SG-CUMDA) loss function $L_{SG-CUMDA}$ which aggregates all the individual re-ID loss functions on each domain, as follows:

$$L_{SG-CUMDA}\left(\theta, \left(S, \hat{T}_1, \ldots, \hat{T}_n\right)\right) = L_{ID}(\theta, S) + \sum_{k=1}^{n} L_{ID}\left(\theta, \hat{T}_k\right) \ . \tag{2}$$

3.3. Alleviating the domain gap with domain-specific batch normalization

It is argued that the gap domain can degrade performance Dubourvieux et al. (2021a). The proposed methodology proposes to mitigate it at the level of batch normalization layers.

Batch Normalization (batchnorm) is a widely-used technique to accelerate and improve the training of deep neural networks, by reducing the internal covariate-shift Ioffe and Szegedy (2015). It consists in normalizing the batch after each convolutional or linear layers, using the batch-wise mean and variance of activations, and learnable affine parameters that rescale the features into batch-normalized features.

Prior works highlighted the negative impact on training stage when computing batchnorm statistics with data from different domains Zajkac et al. (2019). Domain-Specific Batch Normalization (DSBN) layers have been proposed to be effective for various domain adaptation problems such as UDA classification Chang et al. (2019a) and UDA re-ID Dubourvieux et al. (2021a). It consists in using domain-specific batchnorm affine parameters and computing domain-specific mean and variance. Other network parameters are still shared and used whatever the domain. f_θ being implemented by a CNN, DSBN layers are used after each convolutional and fully-connected layers.

3.4. Improving pseudo-labels with multi-target automatic source-guided selection of Pseudo-labeling Hyperparameters

Pseudo-labeling UDA approaches are sensitive to the quality of the proposed labeling, which depends on the good tuning of clustering hyperparameters λ. In the context of pedestrian and vehicle re-ID, the ideal λ value called λ^* has been shown to depend on the target dataset distribution in the feature space, as well as the target dataset statistics (e.g. the number of shots per identity) Dubourvieux et al. (2021b). Most of the works that focus on pedestrian and vehicle UDA re-ID reuse the same values empirically tuned for a specific cross-dataset experiment, on all different cross-datasets considered afterward. It has been shown that this can result in significantly reduced performance compared to getting a suitable value Dubourvieux et al. (2021b).

For real world cow-re-ID, because the target is unlabeled, it is impossible to build a labeled validation set to tune this value. Besides, usual λ value used for person re-ID may not translate well to cow re-ID problem, given the particularities of cow datasets (color distribution, viewpoints …). Therefore, we propose to automate the tuning of λ from the labeled data. To do so, we use the HyperParameters Automated by Source & Similarities (HyPASS) algorithm Dubourvieux et al. (2021b). HyPASS was designed and tested for single-target domain pedestrian and vehicle UDA re-ID. It optimizes clustering hyperparameters from the labeled data of the source validation dataset. More concretely, HyPASS estimates by model selection on C_λ, the value λ^* such as $\lambda^* = \arg\max_\lambda \mathcal{Q}(C_\lambda, S^{val})$ where $\mathcal{Q}$ is a clustering quality function and S^{val} a labeled validation set from the source data. It is illustrated in Fig. 1 as source-guided auto HP tuning.

HyPASS-SC for CUMDA: improving the robustness to domain gap. In this paper, we adapt HyPASS to our cow re-ID CUMDA problem, by selecting a specific value λ_k for each target dataset T_k. The PLC defined by Eq. 1, is redefined as a Domain-specific PLC given by:

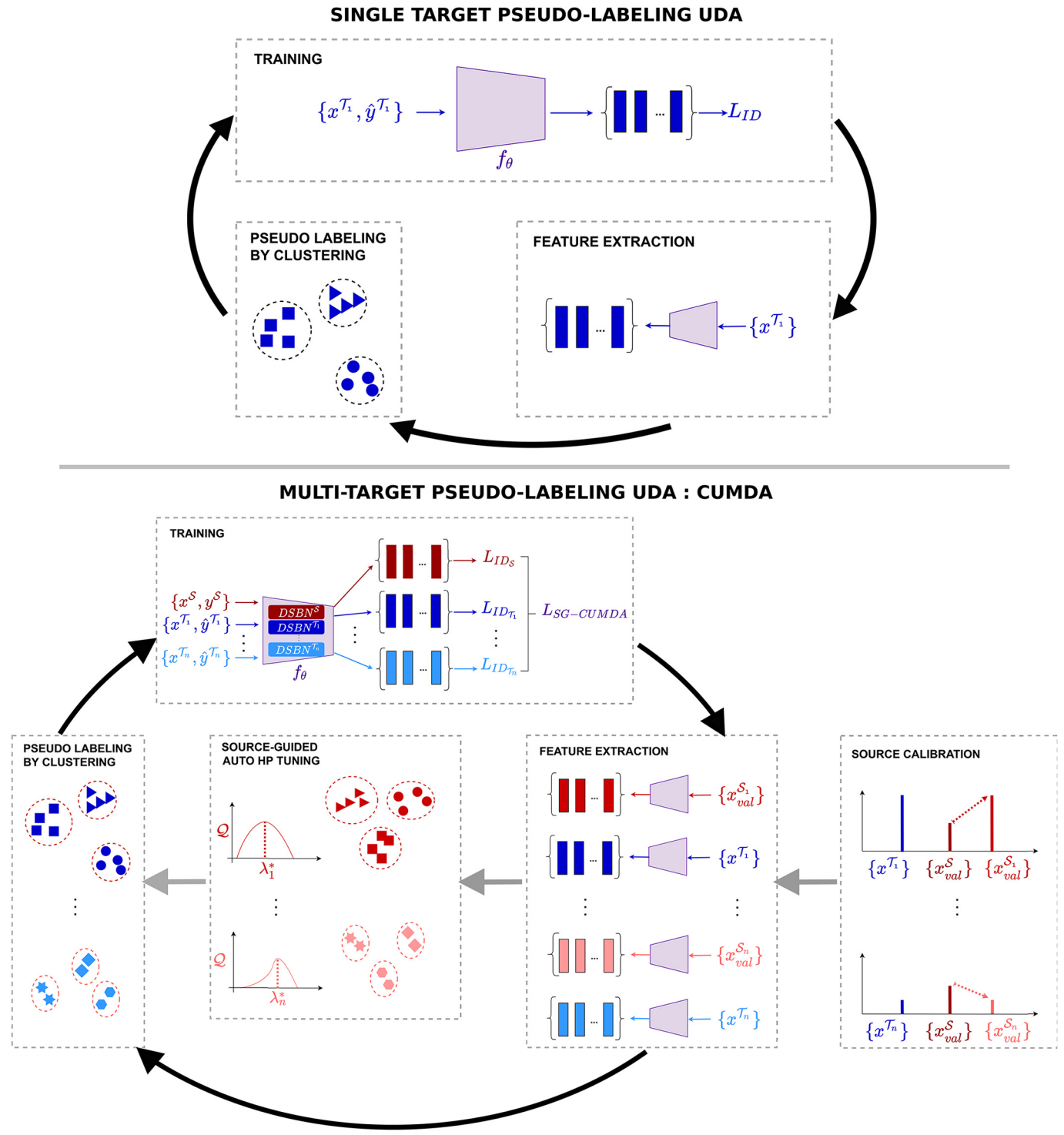

Fig. 1. Upper part: pseudo-labeling paradigm for single-target UDA re-ID. Black arrows indicate the pseudo-labeling and training cycle. *FEATURE EXTRACTION* is carried out for images $\{x^{\mathcal{T}_1}\}$ of the target domain $\mathcal{T}_1$ with a feature encoder f_θ. *PSEUDO LABELING BY CLUSTERING* computes pseudo-labels $\{\hat{y}^{\mathcal{T}_1}\}$ on clustered features. *TRAINING* is done on the pseudo-labeled target set $\{x^{\mathcal{T}_1}, \hat{y}^{\mathcal{T}_1}\}$ by minimizing L_{ID}.

$$\forall k \in [1, n], \widehat{T}_k = C_{\lambda_k}(f_\theta, T_k). \tag{3}$$

HyPASS functioning relies on domain-gap reduction. In the multi-target use-case, we propose to achieve it in two ways:

- At the feature level, target-specific DSBN is leveraged to reduce the domain-gap in the feature space (cf. section 3.3);
- At the dataset statistics level, a new Source validation Calibration (SC) approach is proposed.

While cross-dataset statistic gap may be overlooked for an academic person and vehicle re-ID such as in Dubourvieux et al. (2021b), it becomes crucial in the considered cow re-ID problematic. Indeed, in the well-known person re-ID datasets, usual statistics discrepancies are

minimal, with between 21 and 36 shots per ID (e.g. Market1501 Zheng et al. (2015), DukeMTMC Ristani et al. (2016), personX Sun and Zheng (2019) and MSMT17 Wei et al. (2018b)). However, that does not hold true in all cases. Especially in scarcer animal-related re-ID, where the data may be difficult to acquire, resulting in higher discrepancies in shots per ID. Moreover, contrary to person or vehicle re-ID applications in open-world, the number of cows in a farm of interest is generally known, or can be easily estimated for a cross-domain re-ID applications. This allows us to design SC for cattle re-ID, which consists in equalizing the number of shots per ID of the source to match that of the target. SC generates target-specific source validation sets S_k^{val} from S^{val}, that reduce the cross-dataset statistics gap with the corresponding target training set T_k. SC is represented as Source Calibration on Fig. 1. HyPASS is then run on S_k^{val} to compute λ_k^*, the optimal hyperparameter value for clustering on T_k. The combined use of HyPASS and SC will be referred to as HyPASS-SC in the rest of the paper. Implementation details are given in Sec. 4.2.7.

4. Experiments

4.1. Datasets

In this paper, we employ three different datasets: Cows2021 Gao et al. (2021), HolsteinCattleRecognition Bhole et al. (2019) and the private dataset CowFisheye. The content of each dataset is illustrated in Fig. 2.

4.1.1. Cows2021

Cows2021 Gao et al. (2021) is a dataset featuring RGB images and videos of 186 individuals. The data was acquired from 4 m above the ground by a pinhole camera pointed downwards.

Image extraction. The images were extracted over one month of acquisition. The extraction of cow images from the video stream relies on an oriented bounding-box detector and a tracker. The boxes are centered around cow torsos, excluding their heads, with all individuals facing right. For more details on data acquisition, please refer to Gao et al. (2021).

IDs & samples. In this study, labeled annotations for initial supervised training are needed for relevant performance comparisons with unsupervised UDA. Therefore, only its labeled data is used. A total of 8670 images depicting 181 distinct individuals were extracted, for an average of 48 shots per identity. More details on image repartition can be found in Table 1.

Complexity. Despite an acquisition that spreads over one month, the illumination and viewpoint of the cows vary little between acquisitions. There is little to no occlusion in the images.

4.1.2. HolsteinCattleRecognition

HolsteinCattleRecognition Bhole et al. (2019) is a dataset featuring RGB and infrared images of 1237 individuals. The data was acquired by a pinhole camera placed at gound level, 5 m away from the milking machine it films. For concision, we refer to it as HolsteinCattle in the rest of the paper.

Table 1
Dataset statistics. For Cows2021 Gao et al. (2021) and HolsteinCattle Bhole et al. (2019), *indicates that the dataset is extracted from the RGB annotated portion of the complete dataset, following a 50/50 ID split for Train/Test. There is no overlap between train IDs and test IDs (cf. Sec. 4.2.6).

Dataset	# train IDs	# train images	# test IDs	# query images	# gallery images
Cows2021*	90	4602	91	855	3213
HolsteinCattle*	68	609	68	204	414
CowFisheye	62	6334	16	151	2224

Image extraction. The images were extracted over nine days of acquisition. Each of them contains a single cow in the milking machine. For more details on data acquisition, please refer to Bhole et al. (2019).

IDs & samples. In this study, only the RGB data is used. A total of 1227 images depicting 136 distinct individuals were extracted, for an average of 9 shots per identity. More details on image repartition can be found in Table 1.

Complexity. This dataset features partially occluded cattle positioned differently in the milking machine.

4.1.3. CowFisheye

CowFisheye is a private dataset featuring RGB images of 78 individuals. It was acquired from a single farm from 4 fisheye cameras pointing downwards, positioned 6 m above the ground. Identities were annoted manually. This dataset reflects the usual challenging data encountered in the use case where cows must be identified 24/7 wherever they are in the farm.

Image extraction. Images were extracted over 6 days of acquisition, during both day and night. A detector gives images containing the whole cow body and head, aligned horizontally and facing right.

IDs & samples. Manual selection and annotation of images were done to ensure a good variability of viewpoints and lighting conditions for each cow. A total of 8709 images depicting 78 distinct individuals were extracted for an average of 112 instances per identity. More details on images repartition can be found in Table 1 and Fig. 3.

Complexity. The CowFisheye dataset complexity reflects the desired application: re-ID for 24/7 monitoring of cows in the whole camera network. More precisely, the low angle-shot camera configuration required for coverage of the whole farm, may introduce significant cow occlusion by obstacles or other individuals. Distortions inherent to fisheye cameras are also present. Besides, the acquisition is done in varied illumination conditions, which can cause significant discrepancies in the appearance of a cow. At night specifically, a near-infrared mode is activated resulting in black and white pictures. An illustration of the complexity of the CowFisheye dataset is proposed in Fig. 4.

4.2. Experimental settings

4.2.1. Use case

Our use case is specific to re-ID of animals in multiple farms, with labeled images from one farm, and one or many unlabeled images from multiple farms. The objective of our CUMDA re-ID method presented in Sec. 3 is twofold:

Fig. 2. Illustration of the content of each dataset. From left to right: Cows2021 Gao et al. (2021), HolsteinCattleRecognition Bhole et al. (2019), CowFisheye (private).

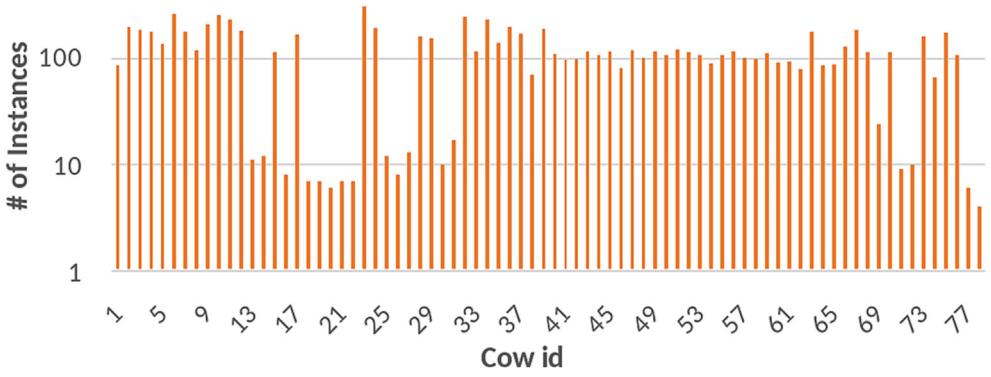

Fig. 3. Number of images per ID in CowFisheye dataset.

- conservation on the source (labeled) domain;
- specialization on the target (unlabeled) domains.

We also expect better generalization on a new unseen target domain which would correspond to a new farm in a real world application.

Therefore, for each training, performance on all three datasets is reported. Throughout the experiments, we evaluate the different components of our CUMDA method: source guidance (cf. Sec. 3.2), DSBN (cf. Sec. 3.3) and HyPASS-SC (cf. Sec. 3.4). Please note that this work does not aim at optimizing the network architecture or tuning hyperparameters, it rather proposes an methodology for efficient CUMDA re-ID by pseudo-labeling.

4.2.2. Framework

In order to introduce some robustness to the pseudo-labels noise, we use the state-of-the-art framework Mutual Mean Teaching (MMT) Ge et al. (2019) paired with a Resnet-18 He et al. (2016) backbone pretrained on ImageNet Deng et al. (2009). The last stride of the Resnet-18 is set to 1 to increase the feature map resolution. The DBSCAN clustering algorithm is run on the k-reciprocal encoded features with $k = 30$. DBSCAN parameters n_{min} and eps are set to $n_{min} = 0.4$ and $eps = 0.6$, their usual values Dubourvieux et al. (2021b). Their values remain constant, except when eps is optimized by HyPASS-SC. All other unspecified values are set similarly to the original MMT paper Ge et al. (2019). The work conducted in this paper is however not limited to MMT and could be applied to any UDA framework.

4.2.3. Data preprocessing

Per domain, mini-batches of size 16 are built with $P = 4$ identities and K = 4 shots per identity. CUMDA batches may vary in size as they are constructed from one mini-batch for the source dataset and one for each target dataset, when applicable. Thus, their size depends on n_{domain}, the number of domains used during training. Here, the batch size is equal to $16 \times n_{domain}$. Images are resized to 128×128 pixels. *Re*-ID related data augmentations such as crop and flip are applied during the training stage. Random erasing was not applied because it experimentally decreased the cow re-ID performance.

4.2.4. Initial supervised pre-training

The network is trained during 20 epochs on each on the chosen source dataset. The learning rate is set to $lr = 3.5.10^{-4}$. Both triplet and cross-entropy losses are used during the training on source images Ge et al. (2019).

4.2.5. Domain adaptation

The network is trained during 15 epochs of 200 iterations. This choice is driven to avoid overfitting on the smaller datasets. The learning rate is set to $lr = 3.5.10^{-4}$. Both triplet and cross-entropy losses are used during the training. Source and target share the same fully connected layer for classification. When using MMT, testing is systematically done on model number 1 as in real-world applications since determining which model performs best on the target is impossible. Indeed, the target dataset is not annotated. Concerning the adaptation on multiple target datasets, when applicable, DSBN is generalized so as to have one Batch Normalization (BN) per domain. During testing, the BN of the domain that is most similar in appearance to the tested domain is used. More specifically, the test domain BN is used if it has been computed during training. Otherwise, the BN of CowFisheye is used when testing on Cows2021 or HolsteinCattle, and the BN of Cows2021 is used when testing on CowFisheye.

Fig. 4. Illustration of the complexity of the CowFisheye dataset. Left: varied lighting conditions, Center: occlusion by objects/cows, Right: varied viewpoints. All pictures represent the same individual.

4.2.6. Testing

Because most datasets are extracted from a unique camera, the evaluation is done without filtering images from the same camera. The mean Average Precision (mAP) is reported as evaluation metric. It is an indicator of the network ability to correctly recall the different shots in a gallery corresponding to a query individual, and should be maximized.

For completeness sake, rank-1 is also reported in Appendix A. It indicates the accuracy of the rank-1 proposal for each query individual and is representative of the retrieval performance. However, rank-1 is sensitive to shortcomings in the dataset that are especially present in the studied cattle re-id use case (low diversity of images, noise etc.). Therefore, all in text analysis will be made on mAP as it is more robust and representative of the performance on the whole dataset.

No re-ranking is applied during testing. The ID splitting for Cows2021 and HolsteinCattle, is done following the original ascending numbering. The first half of the identities is taken as train set and the other half as test set.

4.2.7. HyPASS-SC

HyPASS-SC optimizes the value of DBSCAN hyperparameter *eps* in the range $[0.35, 0.65]$, which is the range of acceptable values for human datasets applications Dubourvieux et al. (2021b). There is an order of magnitude difference in number of shots per individual between HolsteinCattle (9) and other datasets (48 and 112). Therefore, when dealing with HolsteinCattle as target or as source, HyPASS-SC resp. computes a subsampled or oversampled source validation dataset resp., so that the number of shots per identity in the source validation set roughly matches the one of the target, as described in Sec. 3.4. Impact on the performance of shots leveling will be shown in section 5.3. Random subsampling Cows2021 or CowFisheye is straightforward, while oversampling HolsteinCattle is done by applying the same data augmentation than for training. Please note that the source data used for training is not impacted by this step. In a real-world application, the number of cows in a farm is known and the number of instances per identity can be approximated by dividing the number of acquired images by the estimated number of cows in the exploitation.

5. Results

All results presented below are derived from the experiments detailed in Appendix A. Both mAP and rank-1 metrics are reported in Tables A.11 - A.16, however, only mAP related results are discussed below cf. section 4.2.6.

5.1. Effectiveness of our CUMDA, single target

Supervised training & direct transfer. Supervised training results can be found in Table 2. These results, when training and testing on the same dataset, give an idea of the complexity of each dataset. From highest to lowest: CowFisheye, HolsteinCattle and Cows2021.

We also show the cross-domain performance of models supervised on a source dataset and directly evaluated on the other datasets, without adaptation. The low performance on these datasets demonstrates the need for domain adaptation. In Table 2, two cross-domain experiments stand out. First, the direct transfer Cows2021→ HolsteinCattle shows the poorest performance on the target domain at 8.0% mAP vs the 81.2% which can be attained if annotations were available. Second, the direct transfer CowFisheye→ Cows2021 shows the highest performance of all cross-domain experiments, with 71.0% mAP on the target dataset. These results indicate that the domain gap between farms greatly influences the network ability to perform on a new style of images and is higher between HolsteinCattle and the other datasets than between CowFisheye and Cows2021. Also, the abundance of information present in CowFisheye with its varied viewpoints and occultations helps bridge the gap with other domains as shown by higher direct transfer scores when pre-training on CowFisheye.

UDA baseline. In the rest of the paper, we will refer to domain adaptation without source guidance as UDA. Its functioning is illustrated in the upper part of Fig. 1. We remind the reader that the MMT framework has been chosen as baseline here Ge et al. (2019) and could be replaced by any other baseline as shown in Dubourvieux et al. (2021b) and Dubourvieux et al. (2022).

As shown in Table 3, the performance on the target dataset increases with Δ_{mAP} values in the range $[+1.7$ p.p., $+55.5$ p.p.], meaning a lower bound for performance variation of $+1.7$ percentage points (p.p.) and an upper bound of $+55.5$ p.p.. This shows that the domain adaptation is efficient on the target dataset for all presented cases. However, the decrease seen in all diagonal elements of Table 3, indicates that the source dataset is partially forgotten by the network. This effect is drastic with Δ_{mAP} values in the range $[-61.6$ p.p., -11.2 p.p.].

The generalization performance on an unseen dataset is inconsistent and seems to evolve towards that of a supervised network that is supervised on the target dataset. For example, in the case CowFisheye→ HolsteinCattle, the performance of the network on Cows2021 decreases from 71.0% mAP (cf. Table 2) before UDA to 30.8% mAP after (cf. Table 3). This performance ressembles the 29.1% mAP performance seen for a network solely supervised on HolsteinCattle (cf. Table 2). In conclusion, the UDA approach adapts the network to a single dataset, without ensuring performance gains on any other dataset.

CUMDA. In the rest of the paper, we will refer to domain adaptation with source guidance, DSBN and HyPASS-SC as CUMDA. Its functioning is illustrated in the lower part of Fig. 1. The results with CUMDA are reported in Table 4. The improvements over UDA (cf. Table 3) are multiple.

First, it outperforms the supervised network on source, target and a third unseen domain in a consistent way. On the source domain, the performance is equivalent or better, with a $+9.6$ p.p. increase in terms of mAP for CowFisheye. On the target domain, the performance increase is drastic with an average Δ_{mAP} of $+38.9$ p.p., $+16.5$ p.p. and $+7.8$ p.p. on Cows2021, HolsteinCattle and CowFisheye when they are taken as target domains respectively. Generalization performance on the unseen domain increases on average of $+14.4$ p.p., $+2.7$ p.p. and $+3.0$ p.p. on the same datasets.

Second, on the target domain, our proposed CUMDA method outperforms the UDA. To characterize this, we compute the increment in performance between Tables 4 and 3. On the source domain, the performance increase is drastic with values as high as $81.1 - 19.6 = +61.5$ p.p. for the cross domain HolsteinCattle→ CowFisheye. On the target

Table 2
Performance (mAP in % and accuracy in % of the rank-1 closest element in the gallery) of models supervised on a single source dataset and direct transfer on each target dataset without adaptation.

Method	Train		Test					
	Source	Target	Cows2021		HolsteinCattle		CowFisheye	
			mAP	rank-1	mAP	rank-1	mAP	rank-1
Supervised training	Cows2021	None	**95.3**	**98.2**	8.0	13.7	16.8	45.7
Supervised training	HolsteinCattle	None	29.1	73.1	**81.2**	**91.7**	12.7	25.2
Supervised training	CowFisheye	None	71.0	95.1	13.6	24.5	**50.5**	**75.5**

Table 3
Performance of MMT Ge et al. (2019). mAP (in %), Δ_{mAP} (in p.p.) indicates the difference with initial supervised models (cf Table 2).

Method	Train		Test					
	Source	Target	Cows2021		HolsteinCattle		CowFisheye	
			mAP	Δ_{mAP}	mAP	Δ_{mAP}	mAP	Δ_{mAP}
UDA	Cows2021	HolsteinCattle	39.2	*−56.1*	12.6	**+4.6**	9.1	*−7.7*
UDA	Cows2021	CowFisheye	84.1	*−11.2*	10.8	**+2.8**	24.3	**+7.5**
UDA	HolsteinCattle	Cows2021	84.6	**+55.5**	25.5	*−55.7*	16.0	**+3.3**
UDA	HolsteinCattle	CowFisheye	54.9	**+25.8**	19.6	*−61.6*	14.4	**+1.7**
UDA	CowFisheye	Cows2021	88.9	**+17.9**	8.5	*−5.1*	19.9	*−30.6*
UDA	CowFisheye	HolsteinCattle	30.8	*−40.2*	22.7	**+9.1**	14.3	*−36.2*

Table 4
Performance of our CUMDA method (source guidance, DSBN and HyPASS-SC). mAP (in %), Δ_{mAP} (in p.p.) indicates the difference with initial supervised models (cf Table 2).

Method	Train		Test					
	Source	Target	Cows2021		HolsteinCattle		CowFisheye	
			mAP	Δ_{mAP}	mAP	Δ_{mAP}	mAP	Δ_{mAP}
CUMDA	Cows2021	HolsteinCattle	95.4	+0.1	15.9	**+7.9**	20.1	**+3.3**
CUMDA	Cows2021	CowFisheye	95.0	−0.3	13.7	**+5.7**	28.2	**+11.4**
CUMDA	HolsteinCattle	Cows2021	87.2	**+58.1**	80.8	−0.4	15.3	**+2.6**
CUMDA	HolsteinCattle	CowFisheye	57.9	**+28.8**	81.1	−0.1	16.8	**+4.1**
CUMDA	CowFisheye	Cows2021	90.6	**+19.6**	13.3	−0.3	60.1	**+9.6**
CUMDA	CowFisheye	HolsteinCattle	70.9	−0.1	38.6	**+25.0**	60.1	**+9.6**

domain, the performance increases consistently with values between +1.7 p.p. and + 15.9p.p.. Generalization performance on the unseen domain increases with values between −0.7 p.p. and + 40.1 p.p..

All these results demonstrate the network ability to both remember the source dataset and leverage information from all domains to increase performance steadily on all domains. Our CUMDA method therefore can ensure conservation on the source domain, better specialization on each seen domain and better generalization on unseen domains.

5.2. Ablation study, single target

In section 5.1, we have demonstrated the performance gains brought by our proposed CUMDA method over direct transfer and UDA domain adaptation. In this section, the relative importance of all components of our CUMDA method is investigated through an ablation study. Averaged performance variations with respect to a network supervised on source are reported in Tables 5 - 8. The performance on source, target and a third domain are computed following the protocol presented in Appendix A.2. All results are derived from the experiments detailed in Appendix A, Tables A.11 - A.16. Please be reminded that the components of our CUMDA method refer to the use of source-guidance, DSBN and HyPASS-SC.

Source guidance. Averaged performance with source guidance is reported in Table 6. We compare these results to those of UDA, reported in Table 5.

Providing the source as labeled data during training increases the performance drastically on the source dataset. Compared to regular UDA, the average performance increase is equal to 33.7 − 0.4 = +33.3 p.p., +58.1 p.p. and +42.6 p.p. when considering Cows2021, HolsteinCattle and CowFisheye as source respectively. However, the performance on target dataset is approximately unchanged with an average delta in performance of − 0.1 p.p., − 0.9 p.p. and +1.1 p.p.. The model better generalizes thanks to the knowledge of both source and target domains with an increase of +21.4 p.p., +2.3 p.p. and +5.5 p.p. on Cows2021, HolsteinCattle and CowFisheye respectively.

In summary, compared to UDA, the source guidance allows the model to perform similarly on the target while ensuring good conservation of the source. Benefiting from the information of both source and target, the model better generalizes to an unseen dataset.

DSBN. In this paper, alleviating the domain gap is achieved with the use of DSBN. Averaged performance with source guidance + DSBN is reported in Table 7. We compare these results to those of the source guided approach, reported in Table 6.

When compared to source-guided UDA, there is significant performance increase on the target of 40.2 − 36.6 = +3.6 p.p., +4.0 p.p. and +2.5 p.p. for Cows2021, HolsteinCattle and CowFisheye respectively. However, performance on the source dataset slightly decreases with deltas of +0.7 p.p., − 1.8 p.p. and − 1.7 p.p.. Overall, the generalization to an unseen dataset is unchanged.

In summary, in our experiments, DSBN does not seem to guarantee better cow re-identification. However, we will see that it is useful by allowing the use of HyPASS.

Table 5
Relative performance of UDA, compared to direct transfer. Δ_{mAP} (in p.p.) indicates the difference of mAP (in %) with direct transfer (cf. Table 2).

	Test		
	Cows2021	HolsteinCattle	CowFisheye
Test set as	Δ_{mAP}	Δ_{mAP}	Δ_{mAP}
Source	*−33.7*	*−58.7*	*−33.4*
Target	**+36.7**	**+6.9**	**+4.6**
Unseen	*−7.2*	*−1.2*	*−2.2*

Table 6
Relative performance of source-guided UDA, compared to direct transfer. Δ_{mAP} (in p.p.) indicates the difference of mAP (in %) with direct transfer (cf. Table 2).

	Test		
	Cows2021	HolsteinCattle	CowFisheye
Test set as	Δ_{mAP}	Δ_{mAP}	Δ_{mAP}
Source	−0.4	−0.6	**+9.2**
Target	**+36.6**	**+6.0**	**+5.7**
Unseen	**+14.2**	**+1.1**	**+3.3**

Table 7
Relative performance of source-guided + DSBN UDA, compared to direct transfer. Δ_{mAP} (in p.p.) indicates the difference of mAP (in %) with direct transfer (cf. Table 2).

	Test		
	Cows2021	HolsteinCattle	CowFisheye
Test set as	Δ_{mAP}	Δ_{mAP}	Δ_{mAP}
Source	+0.3	*−2.4*	**+7.5**
Target	**+40.2**	**+10.0**	**+8.2**
Unseen	**+13.0**	**+3.1**	**+2.5**

Table 8
Relative performance of our single target CUMDA, compared to direct transfer. Δ_{mAP} (in p. p.) indicates the difference of mAP (in %) with direct transfer (cf. Table 2).

	Test		
	Cows2021	HolsteinCattle	CowFisheye
Test set as	Δ_{mAP}	Δ_{mAP}	Δ_{mAP}
Source	−0.1	−0.3	**+9.6**
Target	**+38.9**	**+16.5**	**+7.8**
Unseen	**+14.4**	**+2.7**	**+3.0**

HyPASS-SC.

The use of DSBN allows for source-guided selection of pseudo-labeling hyperparameters, achieved here with HyPASS-SC. Averaged performance of UDA with source guidance + DSBN + HyPASS-SC = CUMDA is reported in Table 8. We compare these results to those of the source-guided + DSBN approach, reported in Table 7.

In comparison with source-guided + DSBN UDA, the performance on the target domain HolsteinCattle increases of 16.5 − 10.0 = +6.5 p.p.. This may be explained by the significant differences between HolsteinCattle and other domains, which may result in a significant shift of the optimal value of clustering parameters. On the Cows2021 dataset, HyPASS-SC seems to perform slightly worse than source-guided + DSBN with a difference of − 1.3 p.p.. This seems to indicate that HyPASS-SC may not be optimal in all cases, especially when the source test set has few images. However, HyPASS-SC retains its usage by removing the need for user-set parameters. On the source domain, the performance increases with deltas of − 0.1 − 0.3 = − 0.4 p.p., +2.1 p.p. and +2.1 p.p.. It even exceeds the performance of source-guided UDA (cf. Table 6). The generalization performance is increased of +1.4 p.p., − 0.4 p.p. and +0.5 p.p..

In conclusion, we find that HyPASS-SC has a positive effect on performance on all datasets. Indeed, it ensures good clustering on all targets. This allows for better source conservation, target specialization and generalization on an unseen dataset than the other approaches presented here.

For the cross-domain HolsteinCattle→ CowFisheye, a t-SNE visualization of the effects of domain adaptation, source-guidance and other components of the CUMDA method on the embedding space, is proposed in Fig. 5. It shows: the decreased performance on source with UDA, the increased performance on all datasets with source guidance and the best performances obtained by combining all the components of our CUMDA method.

CUMDA re-ID with multiple-targets (CowFisheye and Cows2021) is also illustrated with clear gains on all three datasets. Quantitative evaluations are presented in Sec. 5.4.

5.3. Benefit of the source calibration in HyPASS-SC

As explained in section 3.4, HyPASS is sensitive to dataset statistics. More specifically, in our case, to the number of shots per identity of Cows2021 (48), HolsteinCattle (9) and CowFisheye (112).

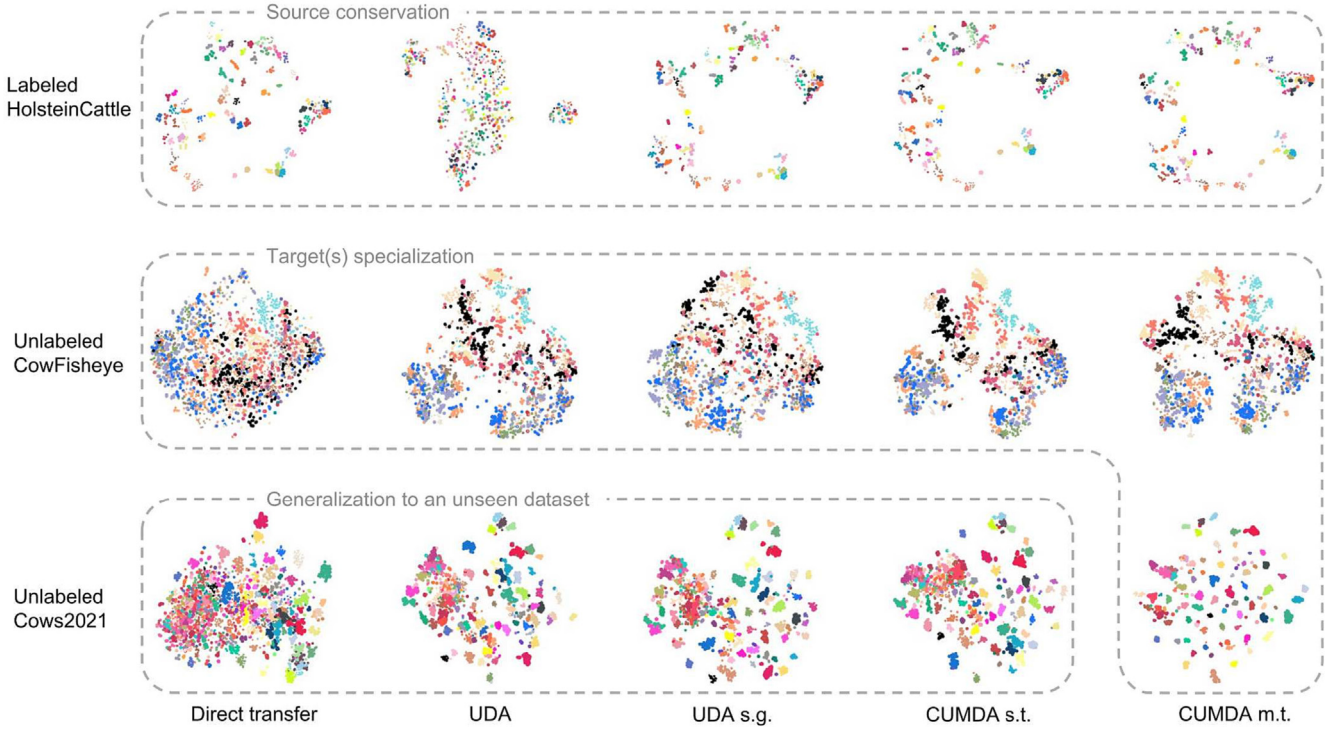

Fig. 5. Evolution of the embedding space on all validation datasets for the cross-domain HolsteinCattle→ CowFisheye. Visualization with t-SNE where each identity is assigned a random color and size. Each point represents an image in the embedding space. Each row corresponds to a dataset. Each column corresponds to a method. Acronyms. **UDA**: UDA baseline with MMT; **s.g.**: source guided; **CUMDA**: Cumulative Unsupervised Multi-Domain Adaptation; **s.t.**: single-target; **m.t.**: multi-target (with Cows2021). Ideally, points of the same colors should be clustered and well separated from all other clusters. Corresponding ranking visualization is available in Fig. A.7 in the appendix. Best viewed in color.

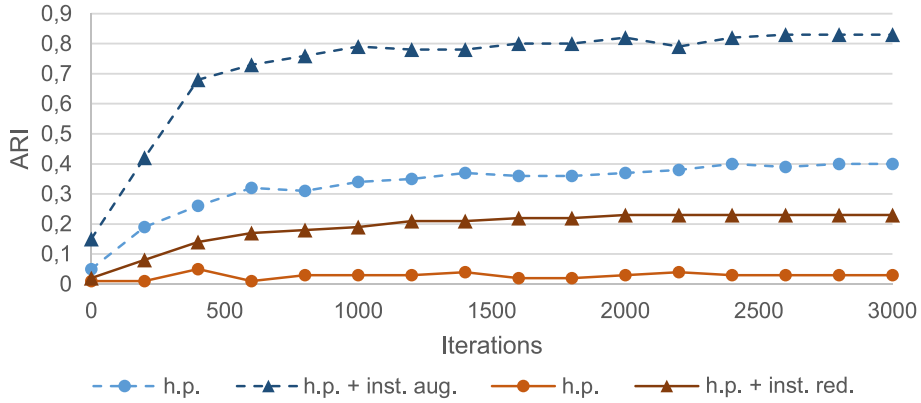

Fig. 6. Evolution of the Adjusted Random Index (ARI) of target clustering. Influence of the calibration of source validation set on HyPASS performances. In blue and dashed lines HolsteinCattle→ Cows2021, in red, CowFisheye→ HolsteinCattle. Acronyms. **h.p.**: HyPASS Dubourvieux et al. (2021b); **inst. Red.**: source instance reduction; **inst. Aug.**: source instance augmentation. (For interpretation of the references to color in this figure legend, the reader is referred to the web version of this article.)

To validate the importance of our proposed source validation set calibration, we compare the performance of HyPASS-SC and HyPASS on the cross domains HolsteinCattle→ Cows2021 (oversampling use-case) and CowFisheye→ HolsteinCattle (subsampling use-case).

The quality of the clustering is evaluated with the Adjusted Random Index (ARI) which is a measure of the similarity between two data clusterings. It is computed between the target training set labels and the cluster predictions, using the scikit-learn implementation[2]. Fig. 6 illustrates the evolution of ARI when leveling the source and target statistics. Higher values of ARI indicate a better clustering. Performance is compared at the 3000^{th} iteration.

In the cross-domain HolsteinCattle→ Cows2021, an oversampling of HolsteinCattle from 9 shots/ID to around 90 shots/ID is carried out. As a result, the ARI doubles, increasing from 0.40 without calibration, to 0.83 with it. In terms of mAP, the performance on the target Cows2021 increases from 77.4% without calibration, to 87.2% with it.

In the cross-domain CowFisheye→ HolsteinCattle, a subsampling of CowFisheye from 112 shots/ID to around 9 shots/ID is carried out. The resulting ARI increase is substantial, evolving from 0.03 without calibration, to 0.23 with it. In terms of mAP, the performance on the target HolsteinCattle increases from 29.3% without calibration, to 38.6% with it.

These results show the importance of source validation set calibration in the case of datasets with highly different number of shots per ID, which can be a recurrent issue when dealing with animal datasets. We kindly remind the reader that the calibration of the source has been systematically applied on all aforementioned experiments.

5.4. Effectiveness of our CUMDA, multiple targets

One of our goals is to generalize the domain adaptation to multiple target domains. This use-case reflects real-world needs where, from a labeled dataset, the model should be adapted to multiple farming exploitations. Averaged performance of our CUMDA approach (source guidance, DSBN and HyPASS-SC) is reported in Table 10. It is computed from the detailed results that can be found in Tables A.11 - A.16 of Appendix A. We compare these results to those of the source-guided approach, reported in Table 9.

On the target datasets, our approach outperforms the source-guided UDA approach with Δ_{mAP} of +2.8 p.p., +6.0 p.p. and +3.7 p.p. for Cows2021, HolsteinCattle and CowFisheye respectively. Besides, the performance on the source dataset is conserved. This demonstrates the importance of the proposed CUMDA method when it comes to multiple datasets application. This performance increase can be explained by the complementarity of DSBN and HyPASS-SC.

DSBN allows some domain gap alleviation through domain specific normalization. It also authorizes domains to share the same backbone, which helps generalization. HyPASS-SC provides optimized clustering parameters on each target dataset, depending on its statistics. This ensures good clustering quality on the target domains, which in turn increases the network performance on all datasets.

5.5. Limitations

In this paper, we have shown significant improvements on unsupervised domain adaptation performance when compared with traditional pseudo-labelling-based UDA methods. However, it can be seen that the performance on a domain when it is unlabeled, taken as a target, remains far from the performance on the same domain when it is labeled, taken as a source.

This is a peculiarity of the cow re-ID problem. Indeed, color information usually facilitates the pseudo-labeling in human re-ID and the performance of unsupervised UDA is close to the performance of supervised training Ge et al. (2019). For cow re-ID, color does not contain relevant information for pseudo-labeling. Therefore, subtle information such as shape has to be considered instead. Also, in this paper and cow re-ID in general, the domain gap existing between the chosen datasets can be greater than the one usually seen in person re-ID.

In other words, even if the pseudo-labelling hyperparameters are automatically optimized, the proposed solution is still limited by the pseudo-labelling strategy itself. Namely, pseudo-labels quality depend on the the chosen clustering algorithm, and the networks ability to extract discriminative representations. Detailed discussion on the influence of pseudo-labelling methods on UDA can be found in Dubourvieux et al. (2021b).

Table 9
Relative performance of source-guided + multi-target UDA, compared to direct transfer. Δ_{mAP} (in p.p.) indicates the difference of mAP (in %) with direct transfer (cf. Table 2).

	Test		
	Cows2021	HolsteinCattle	CowFisheye
Test set as	Δ_{mAP}	Δ_{mAP}	Δ_{mAP}
Source	−0.3	*−1.5*	**+10.5**
Target	**+36.0**	**+7.4**	**+3.8**

[2] https://scikit-learn.org/.

Table 10
Relative performance of our CUMDA method, compared to direct transfer. Δ_{mAP} (in p.p.) indicates the difference of mAP (in %) with direct transfer (cf. Table 2).

	Test		
	Cows2021	HolsteinCattle	CowFisheye
Test set as	Δ_{mAP}	Δ_{mAP}	Δ_{mAP}
Source	0.0	−0.9	**+10.4**
Target	**+38.8**	**+13.4**	**+7.5**

6. Conclusion

In this paper, we have proposed a new CUMDA re-ID method for efficient cumulative multi-domain adaptation motivated by practical cattle re-ID constraints and requirements. This work reflects real-world application needs for a model to perform better on all domains as the number of farms increase but annotation on them is not necessarily available. Indeed, it extends domain adaptation to multiple target domains, with high discrepancies in both target datasets statistics and domain representations, which are challenges often encountered in practical applications. The proposed CUMDA method consists in: source guidance, domain gap reduction and an automatic source-guided hyperparameter selection for clustering based on HyPASS. A source calibration method to increase HyPASS performance on datasets of great diversity, usually encountered in farming applications, has indeed been proposed. We have compared our solution to direct transfer, domain adaptation and source-guided domain adaptation. Results show significant performance improvements with better source conservation, target specialization and generalization on unseen domains when compared with classical pseudo-labelling-based UDA methods.

CRediT authorship contribution statement

Fabian Dubourvieux: Conceptualization, Methodology, Software, Validation, Formal analysis, Investigation, Writing – original draft, Visualization. **Guillaume Lapouge**: Conceptualization, Methodology, Software, Validation, Formal analysis, Investigation, Writing – original draft, Visualization. **Angélique Loesch**: Writing – review & editing. **Bertrand Luvison**: Writing – review & editing. **Romaric Audigier**: Writing – review & editing.

Declaration of Competing Interest

The authors declare that they have no known competing financial interests or personal relationships that could have appeared to influence the work reported in this paper.

Acknowledgments

Partial financial support was received from the AIHerd company[b].

This publication was made possible by the use of the FactoryIA supercomputer, financially supported by the Ile-de-France Regional Council.

The CowFisheye dataset was kindly provided by the AIHerd company[b].

Ablation study detail

Appendix A.1. Visualization of predictions

A visualization of the ranking proposed by the re-identification network is proposed in Fig.A.7. The chosen scenario is the HolsteinCattle→ CowFisheye unsupervised domain adaptation, also represented in the embedding space in Fig. 5.

Appendix A.2. Performance computation detailed

In this paper, Tables 5 - 8 exhibit the variation in performance of the network, for each ablation step. The Δ_{mAP} is computed from detailed results in Tables A.11 – A.16 under the following protocol. Let us consider a set of n domains $\mathcal{D}_1$, ..., $\mathcal{D}_n$, and let us test on the domain $\mathcal{D}_i$, $i \in \{1, \ldots, n\}$.

If $\mathcal{D}_i$ is tested as a source, the performance for all cross-domain experiments $\mathcal{D}_i \rightarrow \mathcal{D}_k$, $k \in \{1, \ldots, n\} \setminus \{i\}$, is compared to the network supervised on $\mathcal{D}_i$. The result is then averaged.

If $\mathcal{D}_i$ is tested as a target, the performance for all cross-domain experiments $\mathcal{D}_k \rightarrow \mathcal{D}_i$, $k \in \{1, \ldots, n\} \setminus \{i\}$, is compared to the network supervised on $\mathcal{D}_k$. The result is then averaged.

If $\mathcal{D}_i$ is tested as an unseen dataset, the performance for all cross-domain experiments $\mathcal{D}_k \rightarrow \mathcal{D}_m$, $k, m \in \{1, \ldots, n\} \setminus \{i\}$ with $k \neq m$, is compared to the networked supervised on $\mathcal{D}_k$. The result is then averaged.

For the sake of clarity, let us detail the computation of the first line and first column of Table 5: testing UDA (MMT) on Cows2021 as a source dataset. UDA mAP on Cows2021 as a source is equal to 84.1% and 39.2%, for the cross domains Cows2021→ CowFisheye (cf. Table A.12) and Cows2021→ HolsteinCattle (cf. Table A.14) respectively. A supervised network on Cows2021 has a mAP of 95.3% on Cows2021 (cf. Table 2). Therefore, the Δ_{mAP} is equal to $((84.1 - 95.3) + (39.2 - 95.3))/2 = -33.7$ p.p..

Appendix A.3. All results

Detailed experimental results are reported in Tables A.11-A.16. Each line corresponds to a different method, $+/-$ indicates that an element is added/removed from the line immediately above.

Table A.11
Effects of different domain adaptation strategies on re-ID performances, for cross-domain CowFisheye→ HolsteinCattle. Δ_{mAP} (in p.p.) indicates the difference of mAP (in %) with direct transfer. Rank-1 (in %) is also reported.

Method	Train		Test								
	Source	Target	Cows2021			HolsteinCattle			CowFisheye		
			mAP	Δ_{mAP}	rank-1	mAP	Δ_{mAP}	rank-1	mAP	Δ_{mAP}	rank-1
direct transfer	CowFisheye	None	71.0	0	95.1	13.6	0	24.5	50.5	0	75.5
UDA	CowFisheye	HolsteinCattle	30.8	*−40.2*	72.6	22.7	**+9.1**	38.2	14.3	*−36.2*	31.1
+ source guided	CowFisheye	HolsteinCattle	71.5	+0.5	93.9	25.6	**+12.0**	41.7	59.6	**+9.1**	86.1
+ DSBN	CowFisheye	HolsteinCattle	72.3	**+1.3**	94.5	26.8	**+13.2**	42.2	55.4	**+4.9**	82.1
+ HyPASS-SC	CowFisheye	HolsteinCattle	70.9	−0.1	94.4	38.6	**+25.0**	61.8	60.1	**+9.6**	84.1
+ multi-target	CowFisheye	HolsteinCattle Cows2021	90.8	**+19.8**	98.2	34.5	**+20.9**	54.9	60.9	**+10.4**	85.4
− HyPASS-SC − DSBN	CowFisheye	HolsteinCattle Cows2021	89.2	**+18.2**	97.8	25.3	**+11.7**	44.1	61.0	**+10.5**	84.8

[b] https://www.aiherd.io.

Fig. A.7. Visualization of the ranking performance on all validation datasets for the cross-domain HolsteinCattle→ CowFisheye. For each query, the top 9 results in the gallery are plotted from left to right. Pictures framed in green are correct results, and in red, incorrect ones. The animal identity is plotted on top of each image. Each line corresponds to a use-case. Acronyms. **UDA**: UDA with MMT; **s.g.**: source guided; **CUMDA**: Cumulative Unsupervised Multi-Domain Adaptation; **s.t.**: single-target; **m.t.**: multi-target (with Cows2021). Best viewed in color. (For interpretation of the references to color in this figure legend, the reader is referred to the web version of this article.)

Table A.12
Effects of different domain adaptation strategies on re-ID performances, for cross-domain Cows2021→ CowFisheye. Δ_{mAP} (in p.p.) indicates the difference of mAP (in %) with direct transfer. Rank-1 (in %) is also reported.

Method	Train		Test								
	Source	Target	Cows2021			HolsteinCattle			CowFisheye		
			mAP	Δ_{mAP}	rank-1	mAP	Δ_{mAP}	rank-1	mAP	Δ_{mAP}	rank-1
direct transfer	Cows2021	None	95.3	0	98.2	8.0	0	13.7	16.8	0	45.7
UDA	Cows2021	CowFisheye	84.1	*−11.2*	97.0	10.8	**+2.8**	15.7	24.3	**+7.5**	59.6
+ source guided	Cows2021	CowFisheye	94.9	−0.4	98.6	10.5	**+2.5**	17.2	26.0	**+9.2**	60.9
+ DSBN	Cows2021	CowFisheye	95.1	−0.2	98.5	15.1	**+7.1**	21.1	30.5	**+13.7**	67.5
+ HyPASS-SC	Cows2021	CowFisheye	95.0	−0.3	98.4	13.7	**+5.7**	23.5	28.2	**+11.4**	64.9
+ multi-target	Cows2021	CowFisheye HolsteinCattle	95.3	0.0	98.5	13.8	**+5.8**	24.0	27.2	**+10.4**	66.2
– HyPASS-SC – DSBN	Cows2021	CowFisheye HolsteinCattle	95.0	−0.3	98.4	11.1	**+3.1**	17.6	22.3	**+5.5**	57.0

Table A.13
Effects of different domain adaptation strategies on re-ID performances, for cross-domain HolsteinCattle→ CowFisheye. Δ_{mAP} (in p.p.) indicates the difference of mAP (in %) with direct transfer. Rank-1 (in %) is also reported.

Method	Train		Test								
	Source	Target	Cows2021			HolsteinCattle			CowFisheye		
			mAP	Δ_{mAP}	rank-1	mAP	Δ_{mAP}	rank-1	mAP	Δ_{mAP}	rank-1
direct transfer	HolsteinCattle	None	29.1	0	73.1	81.2	0	91.7	12.7	0	25.2
UDA	HolsteinCattle	CowFisheye	54.9	**+25.8**	90.6	19.6	*−61.6*	31.9	14.4	**+1.7**	37.7
+ source guided	HolsteinCattle	CowFisheye	57.0	**+27.9**	90.5	81.7	+0.5	92.6	14.8	**+2.1**	39.1
+ DSBN	HolsteinCattle	CowFisheye	53.8	**+24.7**	87.6	78.9	*−2.3*	89.2	15.4	**+2.7**	46.4
+ HyPASS-SC	HolsteinCattle	CowFisheye	57.9	**+28.8**	90.8	81.1	−0.1	92.2	16.8	**+4.1**	47.0
+ multi-target	HolsteinCattle	CowFisheye Cows2021	86.8	**+57.7**	97.2	80.3	−0.9	90.7	17.2	**+4.5**	55.6
– HyPASS-SC – DSBN	HolsteinCattle	CowFisheye Cows2021	82.8	**+53.7**	96.6	79.7	*−1.5*	90.7	14.7	**+2.0**	43.0

Table A.14
Effects of different domain adaptation strategies on re-ID performances, for cross-domain Cows2021→ HolsteinCattle. Δ_{mAP} (in p.p.) indicates the difference of mAP (in %) with direct transfer. Rank-1 (in %) is also reported.

Method	Train		Test								
	Source	Target	Cows2021			HolsteinCattle			CowFisheye		
			mAP	Δ_{mAP}	rank-1	mAP	Δ_{mAP}	rank-1	mAP	Δ_{mAP}	rank-1
direct transfer	Cows2021	None	95.3	0	98.2	8.0	0	13.7	16.8	0	45.7
UDA	Cows2021	HolsteinCattle	39.2	*−56.1*	81.5	12.6	**+4.6**	24.0	9.1	*−7.7*	12.6
+ source guided	Cows2021	HolsteinCattle	94.8	−0.5	98.1	7.9	−0.1	18.6	18.9	**+2.1**	53.0
+ DSBN	Cows2021	HolsteinCattle	96.0	+0.7	98.4	14.7	**+6.7**	26.0	19.3	**+2.5**	51.7
+ HyPASS-SC	Cows2021	HolsteinCattle	95.4	+0.1	98.6	15.9	**+7.9**	26.5	20.1	**+3.3**	55.6
+ multi-target	Cows2021	CowFisheye HolsteinCattle	95.3	0.0	98.5	13.8	**+5.8**	24.0	27.2	**+10.4**	66.2
– HyPASS-SC – DSBN	Cows2021	CowFisheye HolsteinCattle	95.0	−0.3	98.4	11.1	**+3.1**	17.6	22.3	**+5.5**	57.0

Table A.15
Effects of different domain adaptation strategies on re-ID performances, for cross-domain CowFisheye→ Cows2021. Δ_{mAP} (in p.p.) indicates the difference of mAP (in %) with direct transfer. Rank-1 (in %) is also reported.

Method	Train		Test								
	Source	Target	Cows2021			HolsteinCattle			CowFisheye		
			mAP	Δ_{mAP}	rank-1	mAP	Δ_{mAP}	rank-1	mAP	Δ_{mAP}	rank-1
direct transfer	CowFisheye	None	71.0	0	95.1	13.6	0	24.5	50.5	0	75.5
UDA	CowFisheye	Cows2021	88.9	**+17.9**	97.8	8.5	*−5.1*	14.2	19.9	*−30.6*	52.3
+ source guided	CowFisheye	Cows2021	89.9	**+18.9**	97.8	13.2	−0.4	23.5	59.8	**+9.3**	82.1
+ DSBN	CowFisheye	Cows2021	91.5	**+20.5**	98.4	12.7	−0.9	22.1	60.6	**+10.1**	88.1
+ HyPASS-SC	CowFisheye	Cows2021	90.6	**+19.6**	98.0	13.3	−0.3	21.1	60.1	**+9.6**	88.1
+ multi-target	CowFisheye	HolsteinCattle Cows2021	90.8	**+19.8**	98.2	34.5	**+20.9**	54.9	60.9	**+10.4**	85.4
– HyPASS-SC – DSBN	CowFisheye	HolsteinCattle Cows2021	89.2	**+18.2**	97.8	25.3	**+11.7**	44.1	61.0	**+10.5**	84.8

Table A.16
Effects of different domain adaptation strategies on re-ID performances, for cross-domain HolsteinCattle→ Cows2021. Δ_{mAP} (in p.p.) indicates the difference of mAP (in %) with direct transfer. Rank-1 (in %) is also reported.

Method	Train		Test								
	Source	Target	Cows2021			HolsteinCattle			CowFisheye		
			mAP	Δ_{mAP}	rank-1	mAP	Δ_{mAP}	rank-1	mAP	Δ_{mAP}	rank-1
direct transfer	HolsteinCattle	None	29.1	0	73.1	81.2	0	91.7	12.7	0	25.2
UDA	HolsteinCattle	Cows2021	84.6	**+55.5**	96.1	25.5	*−55.7*	37.3	16.0	**+3.3**	52.3
+ source guided	HolsteinCattle	Cows2021	83.4	**+54.3**	97.1	79.4	*−1.8*	89.2	17.1	**+4.4**	49.0
+ DSBN	HolsteinCattle	Cows2021	89.0	**+59.9**	98.4	78.8	*−2.4*	87.3	15.2	**+2.5**	47.7
+ HyPASS-SC	HolsteinCattle	Cows2021	87.2	**+58.1**	97.3	80.8	−0.4	90.7	15.3	**+2.6**	49.0
+ multi-target	HolsteinCattle	CowFisheye Cows2021	86.8	**+57.7**	97.2	80.3	−0.9	90.7	17.2	**+4.5**	55.6
– HyPASS-SC – DSBN	HolsteinCattle	CowFisheye Cows2021	82.8	**+53.7**	96.6	79.7	*−1.5*	90.7	14.7	**+2.0**	43.0

References

Andrew, W., Hannuna, S., Campbell, N., Burghardt, T., 2016. Automatic individual Holstein friesian cattle identification via selective local coat pattern matching in rgb-d imagery. IEEE Proc. Int. Conf. Image. Proc. 484–488.

Andrew, W., Greatwood, C., Burghardt, T., 2017. Visual localisation and individual identification of Holstein friesian cattle via deep learning. Proc. IEEE Int. Conf. Comput. Vis. Workshop, pp. 2850–2859.

Andrew, W., Gao, J., Mullan, S., Campbell, N., Dowsey, A.W., Burghardt, T., 2021. Visual identification of individual Holstein-friesian cattle via deep metric learning. Comput. Electron. Agric. 185, 106133.

Bak, S., Carr, P., Lalonde, J.F., 2018. Domain adaptation through synthesis for unsupervised person re-identification. Comput. Vis. ECCV 189–205.

Bergamini, L., Porrello, A., Dondona, A.C., Del Negro, E., Mattioli, M., D'alterio, N., Calderara, S., 2018. Multi-views embedding for cattle re-identification. IEEE International Conference on Signal-Image Technology & Internet-Based Systems, pp. 184–191.

Bhole, A., Falzon, O., Biehl, M., Azzopardi, G., 2019. A computer vision pipeline that uses thermal and rgb images for the recognition of Holstein cattle. Computer Analysis of Images and Patterns. 11679, 108–119.

Chang, W.G., You, T., Seo, S., Kwak, S., Han, B., 2019a. Domain-specific batch normalization for unsupervised domain adaptation. Proc. IEEE Comput. Soc. Conf. Comput. Vis. Pattern Recognit, pp. 7354–7362.

Chang, X., Yang, Y., Xiang, T., Hospedales, T.M., 2019b. Disjoint label space transfer learning with common factorised space. Proc. AAAI Conf. Artif. Intell.

Chen, Y., Zhu, X., Gong, S., 2019. Instance-guided context rendering for cross-domain person re-identification. Proc. IEEE Int. Conf. Comput. Vis, pp. 232–242.

Chen, G., Lu, Y., Lu, J., Zhou, J., 2020. Deep credible metric learning for unsupervised domain adaptation person re-identification. Comput. Vis. ECCV 643–659.

Deng, J., Dong, W., Socher, R., Li, L.J., Li, K., Fei-Fei, L., 2009. Imagenet: a large-scale hierarchical image database. Proc. IEEE Comput. Soc. Conf. Comput. Vis. Pattern Recognit., pp. 248–255

Deng, W., Zheng, L., Ye, Q., Kang, G., Yang, Y., Jiao, J., 2018. Image-image domain adaptation with preserved self-similarity and domain-dissimilarity for person re-identification. Proc. IEEE Comput. Soc. Conf. Comput. Vis. Pattern Recognit, pp. 994–1003.

Dubourvieux, F., Audigier, R., Loesch, A., Ainouz, S., Canu, S., 2021a. a. Unsupervised domain adaptation for person re-identification through source-guided pseudo-labeling. IEEE proc. Int. Conf. Pattern Recogn, pp. 4957–4964.

Dubourvieux, F., Loesch, A., Audigier, R., Ainouz, S., Canu, S., 2021b. b. Improving unsupervised domain adaptive re-identification via source-gided selection of pseudo-labeling hyperparameters. IEEE Access 9, 149780–149795.

Dubourvieux, F., Audigier, R., Loesch, A., Ainouz, S., Canu, S., 2022. A formal approach to good practices in pseudo-labeling for unsupervised domain adaptive re-identification. Comput. Vis. Image Underst. 223, 103527.

Fu, Y., Wei, Y., Wang, G., Zhou, Y., Shi, H., Huang, T.S., 2019. Self-similarity grouping: a simple unsupervised cross domain adaptation approach for person re-identification. Proc. IEEE Int. Conf. Comput. Vis. 6112–6121.

Gao, J., Burghardt, T., Andrew, W., Dowsey, A.W., Campbell, N.W., 2021. Towards self-supervision for video identification of individual holstein-friesian cattle: the Cows2021 dataset. arXiv preprint arXiv:2105.01938.

Ge, Y., Chen, D., Li, H., 2019. Mutual mean-teaching: pseudo label refinery for unsupervised domain adaptation on person re-identification. International Conference on Learning Representations.

Ge, Y., Zhu, F., Chen, D., Zhao, R., Li, H., 2020. Self-paced contrastive learning with hybrid memory for domain adaptive object re-id, in: Adv. Neural. Inf. Process. Syst, pp. 11309–11321.

He, K., Zhang, X., Ren, S., Sun, J., 2016. Deep residual learning for image recognition. Proc. IEEE Comput. Soc. Conf. Comput. Vis. Pattern Recognit, pp. 770–778.

Hermans, A., Beyer, L., Leibe, B., 2017. In defense of the triplet loss for person re-identification. arXiv preprint. arXiv:1703.07737.

Huang, Y., Wu, Q., Xu, J., Zhong, Y., 2019. Sbsgan: suppression of inter-domain background shift for person re-identification. Proc. IEEE Int. Conf. Comput. Vis. 9527–9536.

Ioffe, S., Szegedy, C., 2015. Batch normalization: accelerating deep network training by reducing internal covariate shift. Proc. Int. Conf. Mach. Learn. 448–456.

Jin, X., Lan, C., Zeng, W., Chen, Z., 2020. Global distance-distributions separation for unsupervised person re-identification. Comput. Vis. ECCV 735–751.

Khan, S.D., Ullah, H., 2019. A survey of advances in vision-based vehicle re-identification. Comput. Vis. Image Underst. 182, 50–63.

Krizhevsky, A., Sutskever, I., Hinton, G.E., 2012. Imagenet classification with deep convolutional neural networks. Adv. Neural Inf. Proces. Syst. 25.

Li, Y.J., Yang, F.E., Liu, Y.C., Yeh, Y.Y., Du, X., Frank Wang, Y.C., 2018. Adaptation and re-identification network: an unsupervised deep transfer learning approach to person re-identification. Proc. IEEE Comput. Soc. Conf. Comput. Vis. Pattern Recognit. Workshops, pp. 172–178.

Li, S., Li, J., Tang, H., Qian, R., Lin, W., 2019a. Atrw: a benchmark for amur tiger re-identification in the wild. arXiv preprint. arXiv:1906.05586.

Li, Y.J., Lin, C.S., Lin, Y.B., Wang, Y.C.F., 2019b. Cross-dataset person re-identification via unsupervised pose disentanglement and adaptation. Proc. IEEE Int. Conf. Comput. Vis. 7919–7929.

Lin, S., Li, H., Li, C.T., Kot, A.C., 2018. Multi-task mid-level feature alignment network for unsupervised cross-dataset person re-identification, in: 29th British Machine Vision Conference, BMVC 2018.

Liu, C., Zhang, R., Guo, L., 2019a. Part-pose guided amur tiger re-identification. IEEE/CVF International Conference on Computer Vision Workshops.

Liu, J., Zha, Z.J., Chen, D., Hong, R., Wang, M., 2019b. Adaptive transfer network for cross-domain person re-identification. proc. IEEE Comput. Soc. Conf. Comput. Vis. Pattern Recognit, pp. 7202–7211.

Liu, J., Zha, Z.J., Chen, D., Hong, R., Wang, M., 2019c. Adaptive transfer network for cross-domain person re-identification. Proc. IEEE Comput. Soc. Conf. Comput. Vis. Pattern Recognit, pp. 7202–7211.

Liu, N., Zhao, Q., Zhang, N., Cheng, X., Zhu, J., 2019d. Pose-guided complementary features learning for amur tiger re-identification. IEEE/CVF international conference on computer vision workshops.

Luo, H., Gu, Y., Liao, X., Lai, S., Jiang, W., 2019. Bag of tricks and a strong baseline for deep person re-identification. Proc. IEEE Comput. Soc. Conf. Comput. Vis. Pattern Recognit Workshops.

Luo, C., Song, C., Zhang, Z., 2020. Generalizing person re-identification by camera-aware invariance learning and cross-domain mixup. Comput. Vis. ECCV 224–241.

Peng, J., Wang, Y., Wang, H., Zhang, Z., Fu, X., Wang, M., 2020. Unsupervised vehicle re-identification with progressive adaptation. arXiv preprint. arXiv:2006.11486.

Qi, L., Wang, L., Huo, J., Zhou, L., Shi, Y., Gao, Y., 2019. A novel unsupervised camera-aware domain adaptation framework for person re-identification. Proc. IEEE Int. Conf. Comput. Vis, pp. 8080–8089.

Ristani, E., Solera, F., Zou, R., Cucchiara, R., Tomasi, C., 2016. Performance measures and a data set for multi-target, multi-camera tracking. Comput. Vis. ECCV.

Schneider, S., Taylor, G.W., Kremer, S.C., 2020. Similarity learning networks for animal individual re-identification-beyond the capabilities of a human observer. IEEE Winter Conf. Appl. Comput. Vis. Workshops, pp. 44–52.

Song, L., Wang, C., Zhang, L., Du, B., Zhang, Q., Huang, C., Wang, X., 2020. Unsupervised domain adaptive re-identification: theory and practice. Pattern Recogn. 102, 107173.

Sun, X., Zheng, L., 2019. Dissecting person re-identification from the viewpoint of viewpoint. Proc. IEEE Comput. Soc. Conf. Comput. Vis. Pattern Recognit, pp. 608–617.

Tang, H., Zhao, Y., Lu, H., 2019. Unsupervised person re-identification with iterative self-supervised domain adaptation. Proc. IEEE Comput. Soc. Conf. Comput. Vis. Pattern Recognit. Workshops.

Wang, J., Zhu, X., Gong, S., Li, W., 2018. Transferable joint attribute-identity deep learning for unsupervised person re-identification. Proc. IEEE Comput. Soc. Conf. Comput. Vis. Pattern Recognit, pp. 2275–2284.

Wang, J., Lan, C., Liu, C., Ouyang, Y., Qin, T., 2021. Generalizing to unseen domains: a survey on domain generalization. Inte Joint Conf on Artif Intell 4627–4635.

Wei, L., Zhang, S., Gao, W., Tian, Q., 2018a. Person transfer Gan to bridge domain gap for person re-identification. Proc. IEEE Comput. Soc. Conf. Comput. Vis. Pattern Recognit, pp. 79–88.
Wei, L., Zhang, S., Gao, W., Tian, Q., 2018b. Person transfer Gan to bridge domain gap for person re-identification. Proc. IEEE Comput. Soc. Conf. Comput. Vis. Pattern Recognit, pp. 79–88.
Ye, M., Shen, J., Lin, G., Xiang, T., Shao, L., Hoi, S.C., 2021. Deep learning for person re-identification: a survey and outlook. IEEE Trans. Pattern Anal. Mach. Intell. 44, 2872–2893.
Yu, H.X., Zheng, W.S., Wu, A., Guo, X., Gong, S., Lai, J.H., 2019. Unsupervised person re-identification by soft multilabel learning. Proc. IEEE Comput. Soc. Conf. Comput. Vis. Pattern Recognit, pp. 2148–2157.
Zajkac, M., Zolna, K., Jastrzkebski, S., 2019. Split batch normalization: improving semi-supervised learning under domain shift. arXiv preprint. arXiv:1904.03515.
Zhai, Y., Lu, S., Ye, Q., Shan, X., Chen, J., Ji, R., Tian, Y., 2020a. Ad-cluster: augmented discriminative clustering for domain adaptive person re-identification. Proc. IEEE Comput. Soc. Conf. Comput. Vis. Pattern Recognit, pp. 9021–9030.
Zhai, Y., Ye, Q., Lu, S., Jia, M., Ji, R., Tian, Y., 2020b. Multiple expert brainstorming for domain adaptive person re-identification. Comput. Vis. ECCV 594–611.
Zhang, X., Cao, J., Shen, C., You, M., 2019. Self-training with progressive augmentation for unsupervised cross-domain person re-identification. Proc. IEEE Int. Conf. Comput. Vis. 8222–8231.
Zhao, F., Liao, S., Xie, G.S., Zhao, J., Zhang, K., Shao, L., 2020. Unsupervised domain adaptation with noise resistible mutual-training for person re-identification. Comput. Vis. ECCV 526–544.
Zheng, L., Shen, L., Tian, L., Wang, S., Wang, J., Tian, Q., 2015. Scalable person re-identification: A benchmark. Proc. IEEE Int. Conf. Comput. Vis.
Zheng, L., Yang, Y., Hauptmann, A.G., 2016. Person re-identification: past, present and future. arXiv preprint. arXiv:1610.02984.
Zhong, Z., Zheng, L., Li, S., Yang, Y., 2018. Generalizing a person retrieval model hetero-and homogeneously. Comput. Vis. ECCV 172–188.
Zhong, Z., Zheng, L., Luo, Z., Li, S., Yang, Y., 2019. Invariance matters: exemplar memory for domain adaptive person re-identification. Proc. IEEE Comput. Soc. Conf. Comput. Vis. Pattern Recognit, pp. 598–607.
Zhu, J.Y., Park, T., Isola, P., Efros, A.A., 2017. Unpaired image-to-image translation using cycle-consistent adversarial networks. Proc. IEEE Int. Conf. Comput. Vis. 2223–2232.
Zou, Y., Yang, X., Yu, Z., Kumar, B.V., Kautz, J., 2020. Joint disentangling and adaptation for cross-domain person re-identification. Comput. Vis. ECCV 87–104.